

## Effect of Headgroup on DNA–Cationic Surfactant Interactions<sup>†</sup>

Antara Dasgupta and Prasanta Kumar Das\*

Department of Biological Chemistry, Centre for Advanced Materials, Indian Association for the Cultivation of Science, Jadavpur, Kolkata 700032, India

Rita S. Dias,<sup>\*,‡</sup> Maria G. Miguel,<sup>§</sup> and Björn Lindman<sup>‡,§</sup>

Physical Chemistry I, Lund University, P.O. Box 124, 22100 Lund, Sweden, and Departamento de Química, Universidade de Coimbra, 3004-535 Coimbra, Portugal

Vaibhav M. Jadhav, Muthaiah Gnanamani, and Souvik Maiti\*

Institute for Genomics and Integrative Biology, CSIR, Mall Road, Delhi 110 007, India

Received: December 13, 2006; In Final Form: March 17, 2007

The interaction behavior of DNA with different types of hydroxylated cationic surfactants has been studied. Attention was directed to how the introduction of hydroxyl substituents at the headgroup of the cationic surfactants affects the compaction of DNA. The DNA–cationic surfactant interaction was investigated at different charge ratios by several methods like UV melting, ethidium bromide exclusion, and gel electrophoresis. Studies show that there is a discrete transition in the DNA chain from extended coils (free chain) to a compact form and that this transition does not depend substantially on the architecture of the headgroup. However, the accessibility of DNA to ethidium bromide is preserved to a significantly larger extent for the more hydrophilic surfactants. This was discussed in terms of surfactant packing. Observations are interpreted to reflect that the surfactants with more substituents have a larger headgroup and therefore form smaller micellar aggregates; these higher curvature aggregates lead to a less efficient, “patch-like” coverage of DNA. The more hydrophilic surfactants also presented a significantly lower cytotoxicity, which is important for biotechnological applications.

### Introduction

A comprehensive knowledge of the interaction between DNA and cationic lipid molecules and other cationic agents will aid in the understanding of DNA packaging in the cell nucleus, transfection in mammalian cells, and control of transcription.<sup>1–17</sup> There has been considerable interest in characterizing the nature of the fundamental interactions between cationic agents and DNA, and several general approaches have been designed to unravel such interactions.<sup>18–37</sup> One of the important driving forces in all of these systems is the long-range electrostatic interaction between molecules of opposite charge. Among all of the cationic agents, single tail lipid molecules, i.e., surfactants, have been studied extensively. Most of the work in this regard has focused on the fundamental interactions between DNA and conventional cationic surfactants that are commercially available, like long chain alkyl groups with trimethylammonium ion as the headgroup, and it has mostly explored variations in the length of the hydrophobic tail.<sup>18–22,24,38,39</sup> A large number of studies have been devoted to developing twin tailed cationic lipid (CL) molecules that can be used as *in vitro* and *in vivo* gene transfection agents. This research has looked mainly into the transfection efficiency with respect to the complex composition,

size, structure, and preparation method (see reviews in refs 40 and 41). Of special interest is the study of the relation between the structure of the lipid components and the transfection efficiency. A number of different reports have been presented concerning this aspect. It has been observed, for example, that *in vitro* transfection efficiency drastically varies on changing the headgroup chemistry of the cationic lipid molecules,<sup>42</sup> and that it often increases if the headgroup of the carrier vector contains any hydrophilic moiety like a hydroxyethyl group, glucose group, or oligomeric polyethylene glycol (PEG) group.<sup>42,43</sup> However, the physical basis of this kind of enhancement of efficiency due to addition of a hydrophilic group in the headgroup region of the carrier lipid molecules is not clear.

One of the important aspects of gene therapy is suggested to be the charge density of the liposomes used for the formation of lamellar CL–DNA complexes, independently of the internal structure of the lipids used.<sup>44,45</sup> Another important factor for the transfection efficiency is the structure of the formed complexes, especially if the composition is not optimized. The efficiency of the transfection is not only dependent on the entrance of the complex into the cell but also the escape of the complexes from the endosomal membrane. This is believed to be attained by fusion with the CL–DNA complexes and release of smaller complexes or naked DNA into the cytoplasm. For lamellar complexes, this can be achieved for membrane charge densities that are sufficiently high.<sup>44,45</sup> Inverted hexagonal structures are very efficient in releasing the DNA into the cell since these structures are much more prone to fusion.<sup>45</sup>

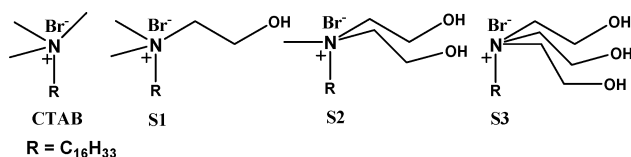
<sup>†</sup> Part of the special issue “International Symposium on Polyelectrolytes (2006)”.

\* To whom correspondence should be addressed. E-mail: bcpkd@iacs.res.in. Fax: +91 33 24732805 (P.K.D.); E-mail: Rita.Dias@fkem1.lu.se. Fax: +46 46 2224413 (R.S.D.); E-mail: souvik@igib.res.in. Fax: +91 11 27667471 (S.M).

<sup>‡</sup> Lund University.

<sup>§</sup> Universidade de Coimbra.

## SCHEME 1



With this in mind, one can rationalize that the presence of hydrophilic groups in the headgroups of the lipids can induce changes in terms of lipid packing that can lead to substantial differences in the self-assembly structures that are formed, when compared with similar lipids without those groups. Also they can, if sufficiently long, provide stability in serum and avoid the aggregation of the CL–DNA complexes due to steric repulsion. This can be achieved by, for example, adding PEG-lipids to the liposome formulation.<sup>46,47</sup>

The information on how the architecture and hydrophilicity of the lipid headgroups influence the interactions with DNA is of fundamental interest and there is a need for rationalization based on systematic studies. However, such biophysical studies demand substantial amounts of the lipid molecules. Unfortunately, synthesis of the twin chain lipid molecules in larger quantities is not an easy task. Single chain cationic surfactants with similar headgroup architecture should be able to serve this purpose, as they are good mimics of the double chain cationic lipid molecules that are used as gene carriers. Incidentally, the synthesis of single chain surfactants with varying headgroup chemistry is relatively easier than that of double tailed lipids.

With this rationale in mind, we sought to synthesize three surfactants by sequential replacement of the  $-CH_3$  groups in cetyltrimethylammonium bromide (CTAB) by hydroxyethyl groups at the surfactant head (surfactants S1–S3 in Scheme 1). The present paper deals with the investigation of the interaction potency of these surfactants having varied hydrophilicity at the headgroup with DNA, at different mole ratios of surfactant/DNA. The extent of the influence of the surfactant's headgroup chemistry on DNA–cationic surfactant interactions was determined by melting transition temperatures, fluorescence spectroscopy, and gel electrophoresis measurements of surfactant/DNA complexes at different mole ratios.

## Materials and Methods

**Materials.** Highly sonicated calf thymus DNA (CT-DNA) from Bangalore Genie, India, was used as received. The size of DNA is between 2 and 2.5 kbp as determined by gel electrophoresis. For the gel electrophoresis experiments performed with the DNA–surfactant complexes, and for better clarity, a linearized form of plasmid DNA (2.6 kb) was used. pUC19 plasmid was isolated from DH5- $\alpha$  cells and digested with Hind III restriction endonuclease (BioLabs). Linearized pUC19 was purified using the standard procedure of phenol chloroform extraction. Unless specified, the DNA was dissolved in 10 mM sodium phosphate buffer (pH 7.0). The concentration of the DNA solutions was measured spectrophotometrically considering the molar extinction coefficient of the DNA base pairs to be equal to  $6600 \text{ M}^{-1} \text{ cm}^{-1}$ .<sup>48</sup> The ratio of the absorbance at 260 and 280 was found to be 1.8.

Analytical grade CTAB was obtained from Spectrochem (India). The hydroxyethyl amines (*N,N*-dimethylethanolamine for the synthesis of S1 and *N*-methyl-diethanolamine for S2) were obtained from Aldrich and 1-bromo-hexadecane from SRL, India Ltd. Hexadecylamine and 2-bromoethanol for synthesizing S3 were obtained from SRL, India Ltd. and Lancaster, U.K. respectively. Agarose was from Amersham Biosciences. Ethid-

ium bromide (EB) was purchased from Aldrich and used as received. Milli-Q water was used for all the experiments.

**Synthesis of Surfactants.** *N*-Hexadecyl-*N,N*-dimethyl-*N*-(2-hydroxyethyl)ammonium bromide (S1) and *N*-Hexadecyl-*N*-methyl-*N,N*-bis(2-hydroxyethyl)ammonium bromide (S2). Both the amphiphiles were prepared following the procedure mentioned in a recently published protocol.<sup>49</sup> Briefly, 1-bromohexadecane and the corresponding amines (*N*-methyl-diethanolamine for S2 and *N,N*-dimethylethanolamine for S1) were taken in the molar ratio 1.2:1 in 30% methanol/acetonitrile and refluxed. After 24 h of refluxing, the solvent was evaporated in rotary evaporator and pure products were obtained by crystallization of the reaction mixture from methanol/ethyl acetate. The yields were 87% and 80% respectively for S1 and S2. **<sup>1</sup>H NMR of S1 (300 MHz, CDCl<sub>3</sub>):**  $\delta$ /ppm = 4.14 [br, 2H, (CH<sub>3</sub>)<sub>2</sub>(HOCH<sub>2</sub>-CH<sub>2</sub>)N<sup>+</sup>(CH<sub>2</sub>-CH<sub>2</sub>-)]; 3.69 [br, 2H, (CH<sub>3</sub>)<sub>2</sub>(HOCH<sub>2</sub>-CH<sub>2</sub>)N<sup>+</sup>(CH<sub>2</sub>-CH<sub>2</sub>-)]; 3.48–3.45 [br, 2H, (CH<sub>3</sub>)<sub>2</sub>(HOCH<sub>2</sub>-CH<sub>2</sub>)N<sup>+</sup>(CH<sub>2</sub>-CH<sub>2</sub>-)]; 3.41 [s, 6H, (CH<sub>3</sub>)<sub>2</sub>(HOCH<sub>2</sub>-CH<sub>2</sub>)N<sup>+</sup>(CH<sub>2</sub>-CH<sub>2</sub>-)]; 1.77 [br, 2H, (CH<sub>3</sub>)<sub>2</sub>(HOCH<sub>2</sub>-CH<sub>2</sub>)N<sup>+</sup>(CH<sub>2</sub>-CH<sub>2</sub>-)]; 1.33–1.18 [br, m, 26H, -(CH<sub>2</sub>)<sub>13</sub>-]; 0.86 [t, 3H, -(CH<sub>2</sub>)<sub>n</sub>CH<sub>3</sub>]. E.A : calculated for C<sub>20</sub>H<sub>44</sub>BrNO: C, 60.89; H, 11.24; N, 3.55. Found: C, 60.85; H, 11.16; N, 3.39. MS (LSIMS) m/z. calcd (for C<sub>20</sub>H<sub>44</sub>NO the 4° ammonium ion, 100%) 314, found 314 (M<sup>+</sup>). **<sup>1</sup>H NMR of S2 (300 MHz, CDCl<sub>3</sub>):**  $\delta$ /ppm = 4.13 [br, 4H, (CH<sub>3</sub>)(HOCH<sub>2</sub>-CH<sub>2</sub>)<sub>2</sub>N<sup>+</sup>(CH<sub>2</sub>-CH<sub>2</sub>-)]; 3.71 [br, 4H, (CH<sub>3</sub>)(HOCH<sub>2</sub>-CH<sub>2</sub>)<sub>2</sub>N<sup>+</sup>(CH<sub>2</sub>-CH<sub>2</sub>-)]; 3.49 [br, 2H, (CH<sub>3</sub>)(HOCH<sub>2</sub>-CH<sub>2</sub>)<sub>2</sub>N<sup>+</sup>(CH<sub>2</sub>-CH<sub>2</sub>-)]; 3.31 [s, 3H, (CH<sub>3</sub>)(HOCH<sub>2</sub>-CH<sub>2</sub>)<sub>2</sub>N<sup>+</sup>(CH<sub>2</sub>-CH<sub>2</sub>-)]; 1.75 [br, 2H, (CH<sub>3</sub>)(HOCH<sub>2</sub>-CH<sub>2</sub>)<sub>2</sub>N<sup>+</sup>(CH<sub>2</sub>-CH<sub>2</sub>-)]; 1.36–1.18 [br, m, 26H, -(CH<sub>2</sub>)<sub>13</sub>-]; 0.88 [t, 3H, -(CH<sub>2</sub>)<sub>n</sub>CH<sub>3</sub>]. E.A : calculated for C<sub>21</sub>H<sub>46</sub>BrNO<sub>2</sub>: C, 59.42; H, 10.92; N, 3.30. Found : C, 59.45; H, 10.86; N, 3.08. MS (LSIMS) m/z. calcd (for C<sub>21</sub>H<sub>46</sub>NO<sub>2</sub> the 4° ammonium ion, 100%) 344, found 344 (M<sup>+</sup>).

*N*-Hexadecyl-*N,N,N*-tris(2-hydroxyethyl)ammonium Chloride (S3). An aqueous solution of NaOH (2.72 g, 0.068 mol, in 25 mL of doubly distilled water) was added dropwise to a mixture of 2-chloroethanol (6.5 g, 0.081 mol) and hexadecylamine (5 g, 0.027 mol) under refluxing condition. After 24 h of refluxing, the reaction mixture was extracted with chloroform (3 × 50 mL). Chloroform was removed on a rotary evaporator followed by drying under vacuum. The residue was then crystallized from methanol/ethyl acetate and filtered. The resulting mixture showed three spots (with R<sub>f</sub> = 0.55, 0.4, and 0) on thin layer chromatography (TLC) using 25:75 (v/v) methanol:chloroform as the TLC developing solvents. The dried product (with R<sub>f</sub> = 0.55) was purified from the white solid obtained from crystallization, by column chromatography in a 230–400 mesh silica gel column with 7% methanol/chloroform. The yield was 40% (4.4 g). **<sup>1</sup>H NMR of S3 (300 MHz, CDCl<sub>3</sub>):**  $\delta$ /ppm = 4.05 [br, 6H, (OHCH<sub>2</sub>-CH<sub>2</sub>)<sub>3</sub>N<sup>+</sup>(CH<sub>2</sub>-CH<sub>2</sub>-)]; 3.48–3.34 [br, 6H, (OHCH<sub>2</sub>-CH<sub>2</sub>)<sub>3</sub>N<sup>+</sup>(CH<sub>2</sub>-CH<sub>2</sub>-)]; 3.23–3.19 [br, 2H, (OHCH<sub>2</sub>-CH<sub>2</sub>)<sub>3</sub>N<sup>+</sup>(CH<sub>2</sub>-CH<sub>2</sub>-)]; 1.84 [br, 2H, (OHCH<sub>2</sub>-CH<sub>2</sub>)<sub>3</sub>N<sup>+</sup>(CH<sub>2</sub>-CH<sub>2</sub>-)]; 1.34–1.19 [br, m, -(CH<sub>2</sub>)<sub>13</sub>-]; 0.88 [t, 3H, -(CH<sub>2</sub>)<sub>n</sub>CH<sub>3</sub>]. E.A: calculated for C<sub>22</sub>H<sub>48</sub>ClNO<sub>3</sub>: C, 64.44; H, 11.80; N, 3.42. Found: C, 64.37; H, 12.10; N, 3.50. MS (LSIMS) m/z. calcd (for C<sub>22</sub>H<sub>48</sub>NO<sub>3</sub> the 4° ammonium ion, 100%) 374, found 330 [(M-CH<sub>2</sub>CH<sub>2</sub>OH+H)<sup>+</sup>].

**Surface Tension Method.** The critical micelle concentration (cmc) values of the surfactants were measured using a tensiometer (Jencon, India) applying the Du Noüy ring method at  $25 \pm 0.1$  °C in water. A 20 mM aqueous solution of the surfactant was made in a 2 mL volumetric flask. The surface tension of 20 mL of pure water in a glass vessel was noted. The surface tension was then measured in varying concentrations

of surfactant solution by adding desired volumes of the stock solution, until there were no observable changes. The cmc values were determined by plotting surface tension ( $\gamma$ ) versus the concentration of surfactant. Each experiment was performed twice, and the results were within  $\pm 2\%$ .

**Determination of Melting Curves of the DNA–Surfactant Complexes.** DNA was dissolved in buffer to a final concentration of 80  $\mu\text{M}$  in phosphate. Different volumes of surfactant solutions were separately added to a constant volume of DNA solution to obtain surfactant/DNA complexes of different charge ratios. After 2 h of incubation at room temperature, the melting profiles of the complexes were obtained by monitoring the absorbance of the complexes at 260 nm as a function of temperature. The samples were heated from 40 to 90  $^{\circ}\text{C}$  at a scanning rate of 1.0  $^{\circ}\text{C}/\text{min}$ . Transition temperatures ( $T_m$ ) were calculated from the melting curves in order to gain insight into the helix–coil transition.

**Ethidium Bromide Exclusion Assay.** Ethidium bromide (EB, 5  $\mu\text{M}$ ) and a 10  $\mu\text{M}$  (one EB per base pair) DNA solution were mixed and allowed to incubate at 25  $^{\circ}\text{C}$  for 10 min. Various amounts of surfactant solutions were added to the DNA–ethidium bromide mixture and then incubated for 30 min. The fluorescence intensity was measured using a spectrofluorometer (FluoroMax-3, Spex) after diluting to 2 mL with 10 mM phosphate buffer. The excitation ( $\lambda_{\text{ex}}$ ) and emission ( $\lambda_{\text{em}}$ ) wavelengths were 480 and 600 nm, respectively.

**Gel Electrophoresis.** The electrophoretic mobility of the cationic surfactant/DNA complexes at different surfactant/DNA ratios was determined by gel electrophoresis using 1.0% agarose gel in TBE buffer (45 mM Tris-borate and 1 mM EDTA at pH 8.0). Experiments were run at 80 V for 90 min. About 40  $\mu\text{g}/\text{mL}$  (equivalent to 121  $\mu\text{M}$  in terms of negative charge) of linearized DNA was mixed with different amounts of surfactant solutions to achieve the desired charge ratio; solutions were incubated for 1 h prior to running the experiment. DNA was visualized under UV illumination by staining the gels with ethidium bromide at room temperature.

**Cytotoxicity Measurements.** HeLa cell line was obtained from NCCS, Pune, India and grown in MEM media (Gibco-BRL, New York) supplemented with 10% fetal calf serum (Biological Industries, Israel), 2 mM L-glutamine (Sigma), 1 mM sodium pyruvate (Sigma), and antibiotic-antimycotic solution (100 $\times$ )(Sigma) at 37  $^{\circ}\text{C}$  in a humidified incubator with 5%  $\text{CO}_2$ . Cells were detached from the culture flask using trypsin–EDTA (Sigma) when they became 70–80% confluent. The HeLa cells were seeded on a 96-well plate at a density of approximately  $25 \times 10^3$  cells/well. After 24 h of incubation, cationic surfactants (0.1–25  $\mu\text{M}$ ) were added to the appropriate wells and were incubated for 24 h. Subsequently, a methyl thiazol tetrazolium (MTT) assay was performed. A total of 10  $\mu\text{L}$  of 5 mg/mL MTT (Sigma) solution [MTT dissolved in Hank's balanced salt solution (HBSS)] was added to each well and incubated for 4 h. Accumulated formazan crystals were solubilized in DMSO (Sigma) and placed on a shaker for 15 min. The absorbance at 560 and 630 nm was recorded in an ELISA plate reader (Spectra MAX 190, Molecular Devices).

## Results and Discussion

This section is organized as follows. We will start by discussing the effect of the surfactant headgroup chemistry on the surfactant micelle formation and, afterward, on the formation of DNA–cationic surfactant complexes in terms of compaction and protection of DNA. Finally, cytotoxicity studies will be presented and discussed.

**TABLE 1: Critical Micellar Concentration (cmc) Values for CTAB and Hydroxylated Surfactants at 25  $^{\circ}\text{C}$**

compound	cmc (M)
CTAB	$9.2 \times 10^{-4}$
S1	$2.02 \times 10^{-4}$
S2	$1.53 \times 10^{-4}$
S3	$0.36 \times 10^{-4}$

**Influence of the Headgroup on the Surfactant Critical Micellar Concentration.** We started by measuring the critical micellar concentration (cmc) for CTAB and each of the synthesized surfactants (Table 1). The cmc of CTAB was found to be 0.92 mM, which is in good agreement with values published previously in the literature.<sup>50</sup> It can also be seen in Table 1 that the cmc of the synthesized surfactants decreases with the addition of the hydrophilic groups. It might have been expected that the surfactants with more hydrophilic groups would have higher cmc's due to sterical repulsions between surfactants in the micellar aggregate. The decrease in the cmc must be associated with the decrease of the electrostatic repulsions between the surfactant headgroups and suggests that the introduction of the hydroxyethyl groups does shield the positive charge in the surfactant headgroup. We can note that insertion of alcohols into ionic surfactant micelles stabilizes the micelles,<sup>51</sup> and that it has been observed for anionic surfactants that the introduction of an oxyethylene group between the alkyl chain and the ionic group reduces the cmc.<sup>52</sup>

**Influence of the Surfactant Headgroup on DNA–Surfactant Complexation.** UV-melting determinations were performed on DNA solutions in the presence and absence of surfactants. This method has been widely used for the characterization of other cationic agents/DNA complexes.<sup>18,28,29,34</sup> Melting is conveniently monitored by an increase in the absorbance (hyperchromic effect) resulting from the disruption of base stacking in double-stranded DNA structure when the double-helix undergoes denaturation. Figure 1 shows the representative melting profiles of free DNA (trace 1) and CTAB/DNA complexes at different charge ratios, 0.25, 0.5, 1.5, and 2.5 (traces 2–5, respectively). As expected, the free DNA solution shows a monophasic melting behavior with a melting temperature around 73  $^{\circ}\text{C}$ . Interestingly, when CTAB is added, we observe the appearance of a second melting temperature, shifted to higher temperatures. For sufficiently large concentrations of surfactant, only the second transition is discernible. The biphasic behavior is more obvious in Figure 2, where the melting data is plotted as the derivative of the absorbance at 260 nm with respect to the temperature, for the different surfactants, at different DNA–cationic surfactant mixing ratios,  $R$ . The decrease in the size of the main transition at 73  $^{\circ}\text{C}$  can be clearly seen, whereas a second transition appears for temperatures around 90  $^{\circ}\text{C}$ .

This biphasic melting transition has been observed already in 1966 by Olins and co-authors<sup>53</sup> and later by Inoue and Ando<sup>54</sup> while studying the interaction between DNA and polypeptides. The first melting transition had a melting temperature similar to DNA alone and was ascribed to the helix  $\rightarrow$  coil transition of free DNA molecules (or portions of molecule), whereas the second transition was attributed to the DNA melting inside the complexes, shifted to higher temperatures due to the increase in the stability of the double-helix state of the DNA molecules. The same behavior has also been observed previously for the DNA–CTAB system.<sup>28</sup> In this work, it was suggested that CTAB binds to both single- and double-stranded forms of DNA; however, we believe that the biphasic melting induced by cationic surfactants arises from the same phenomena as sug-

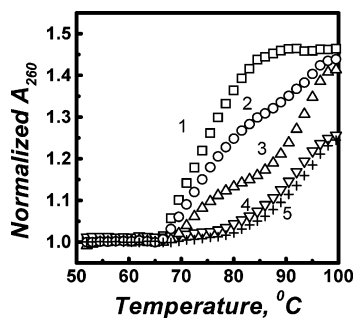


**Figure 1.** Representative UV melting transitions of CT-DNA at 80  $\mu\text{M}$  (in phosphate groups) (trace 1) and of CTAB/CT-DNA complexes at different charge ratios: 0.25, 0.5, 1.5, 2.5, and 5 (traces 2–5, respectively). Experiments performed with 10 mM sodium phosphate buffer (pH 7.0).

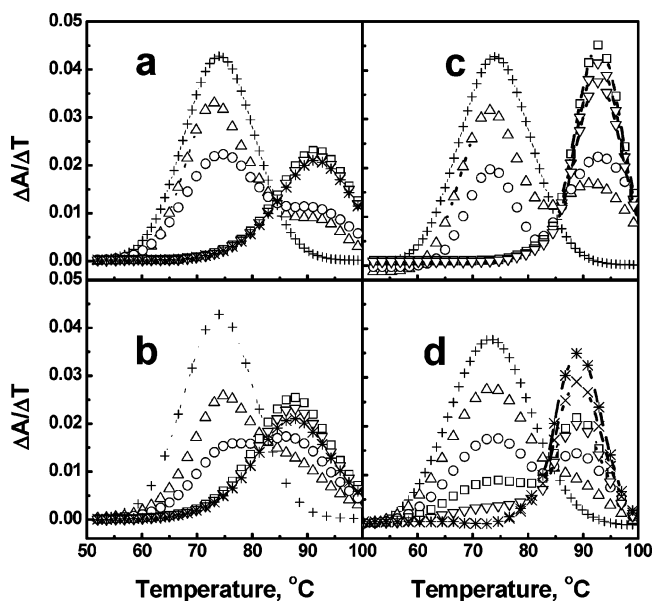


**Figure 2.** Derivative of the absorbance at 260 nm in respect to the temperature,  $\Delta A/\Delta T$ , versus the temperature for (a) CTAB at the charge ratio of 0 (+), 0.25 ( $\Delta$ ), 0.5 ( $\circ$ ), 1.0 ( $\square$ ), 1.5 ( $\nabla$ ), and 3.0 (\*); (b) S1 at the charge ratio of 0 (+), 0.4 ( $\Delta$ ), 0.8 ( $\circ$ ), 1.2 ( $\nabla$ ), 2.0 ( $\square$ ), and 4.0 (\*); (c) S2 at the charge ratio of 0 (+), 0.5 ( $\Delta$ ), 1.0 ( $\circ$ ), 1.5 ( $\nabla$ ), 2.5 ( $\square$ ), and 4.5 (+); and (d) S3 at the charge ratio of 0 (+), 0.25 ( $\Delta$ ), 0.6 ( $\circ$ ), 1.2 ( $\nabla$ ), 2.2 ( $\square$ ), 3.0 ( $\times$ ), and 5.0 (\*).

gested for the polypeptides, that is to the coexistence of DNA molecules that are “naked” (or with insignificant amounts of surfactant bound to them) and DNA molecules complexed with surfactant micelles, where the double-helix is stabilized and persists to higher temperatures. This is in excellent agreement with previous studies by fluorescence microscopy<sup>2</sup> and dynamic light scattering<sup>19,26</sup> experiments where the coexistence of DNA molecules in an extended conformation (coils) and more compacted structures (globules) was clearly observed.

In Figure 3, we compare the melting data for the different surfactants. The open symbols correspond to samples showing the first transition only, i.e., “naked” molecules, the filled symbols show samples with the transition at higher temperatures, where all the DNA molecules are complexed, and the gray symbols represent samples with the two transitions. It can be seen that the appearance of the complexed DNA molecules occurs at around the same concentration for the four surfactants. This indicates that the interaction between DNA and the different cationic surfactants is not dependent on the architecture of the headgroup, per se. This has also been confirmed by fluorescence microscopy, where it was observed that the concentration of

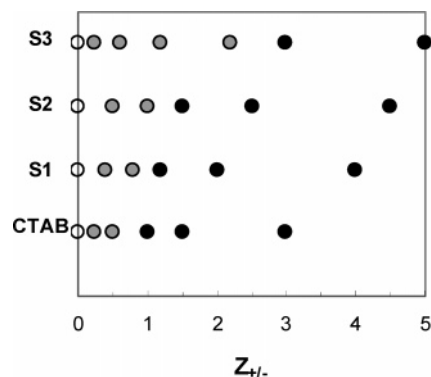


**Figure 3.** Data from the previous figure presented as a conformational map, as function of the charge ratio cationic surfactant–DNA phosphate groups,  $Z_{\pm}$ . The open symbols correspond to samples that present the first transition (at 73  $^{\circ}\text{C}$ ) only, that is, “naked” DNA molecules; filled symbols represent samples where all the DNA is associated into DNA–surfactant complexes, i.e., only the second transition (at 90  $^{\circ}\text{C}$ ) is observed; shaded symbols represent samples that show both transitions.

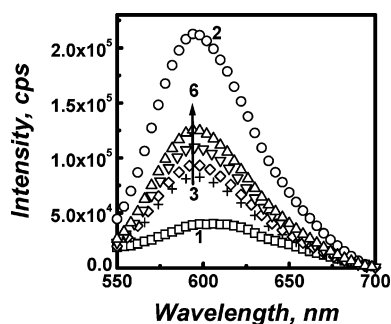


**Figure 4.** Fluorescence emission spectra of EB (trace 1), EB–(CT-DNA) complex (trace 2), and EB–(CT-DNA) complexes in presence of saturated amounts of CTAB (trace 3), S1 (trace 4), S2 (trace 5), S3 (trace 6), respectively. The concentration of CT-DNA was 10  $\mu\text{M}$  in phosphate charges in 10 mM sodium phosphate buffer (pH 7.0).

surfactant required for compacting the first DNA molecules, and for the formation of the last globules (end of the coexistence region), was the same for all the studied surfactants (data not shown, in collaboration with Luís Miguel Magno). Since the compaction of DNA is driven by the formation of surfactant self-assembly, there will be a stronger dependence on the variation of the chain length<sup>20</sup> than on the headgroup architecture. The reason is not clear, however, for the delayed region with complexes alone for the surfactants with more hydroxyethyl groups.

**Surfactant Packing Considerations.** The binding of surfactants to DNA was investigated by fluorescence spectroscopy studies during titrations of the surfactant into a premixed solution of DNA and ethidium bromide (EB). EB is a cationic dye that is widely used as a probe for native DNA. The ethidium ion displays a dramatic increase in fluorescence efficiency when it intercalates into DNA. The displacement of EB from DNA upon complex formation with polycations has been used extensively in the development of nonviral gene delivery systems to detect the interaction of various lipids and polymers with DNA. The addition of cationic agents to premixed DNA-EB solutions will result in the displacement of intercalated EB from the DNA/EB complexes resulting in quenching of fluorescence intensity. Figure 4 shows the fluorescence emission spectra of free EB, the DNA/EB complex, and the spectra after addition of saturating amounts of the four surfactants. Traces 1 and 2 in Figure 4 represent the spectra due to the free ethidium bromide probe and DNA-bound probe, respectively, and traces 3–6 represent the fluorescence spectra obtained upon addition of

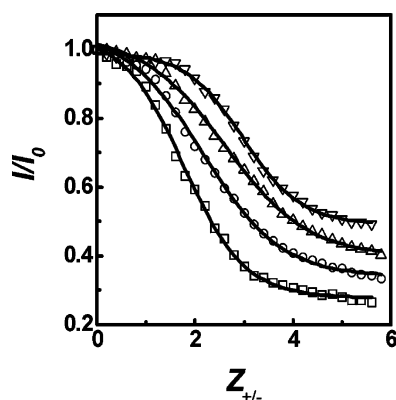


**Figure 5.** Ethidium bromide exclusion experiments for CTAB ( $\square$ ), S1 ( $\circ$ ), S2 ( $\triangle$ ), S3 ( $\nabla$ ), plotted as  $I/I_0$  versus the mixing ratio of cationic surfactant to DNA phosphate groups,  $Z_{\pm}$ . The CT-DNA concentration was  $10 \mu\text{M}$  in phosphate groups in  $10 \text{ mM}$  sodium phosphate buffer (pH 7.0).

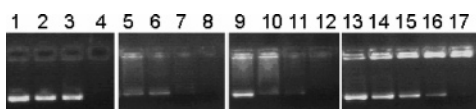


**Figure 6.** Lane 1: free DNA ( $40 \mu\text{g/mL}$ ), lanes 2–4: DNA/CTAB complexes of 0.5, 0.75, and 1.0 charge ratio ( $R$ ) respectively. Lanes 5–8: DNA/S1 complexes with  $R = 0.5, 1.0, 1.5,$  and  $2.0$  charge ratio, respectively. Lanes 9–12: DNA/S2 complexes with  $R = 0.5, 1.0, 1.5,$  and  $2.0$  charge ratio, respectively. Lanes 13–17: DNA/S3 complexes with  $R = 0.5, 1.0, 1.5, 2.0,$  and  $2.5$ , respectively. The experiments were conducted using pUC19 DNA and TBE buffer ( $45 \text{ mM}$  Tris-borate and  $1 \text{ mM}$  EDTA at pH 8.0).

maximum amounts of CTAB, S1, S2, and S3, respectively, into the DNA/EB solution to achieve saturation in the observed fluorescence quenching. Although the fluorescence quenching phenomena were seen in all of the instances, the striking differences lie in the spectrum obtained after achieving saturation. CTAB is able to quench 72% of the initial intensity whereas S1, S2, and S3 are able to quench only 68, 59, and 50%, respectively, of the initial intensity. Typical curves of fluorimetric titrations of solutions of the DNA-EB complex with surfactants of different headgroups are shown in Figure 5. Similar results are confirmed by the gel electrophoresis experiments. Images of agarose gel electrophoresis of a series of surfactant/DNA complexes of different charge ratios are shown in Figure 6. At low charge ratios of surfactant to DNA an excess of uncomplexed DNA was present (a band toward the anode). The migration of plasmid DNA in the gel was retarded as the ratio of surfactant was increased above 1.0, 1.5, 1.5, and 2.5 for CTAB, S1, S2, and S3, respectively, demonstrating that all of the surfactants were capable of binding DNA and neutralizing the charges on the DNA backbone. However, there are subtle differences between the gels for the different surfactants. CTAB neutralizes all of the phosphate groups at a charge ratio of 1.0, but in the presence of the other three surfactants, the DNA still carries a negative net charge at this ratio, as indicated by their migration to the anodic edge of the well.

The differences in the ethidium bromide displacement presented by the different surfactants can be seen in terms of strength of interaction as indicated by the critical association concentration ( $cac$ ) values at which the surfactant starts to bind to DNA or to the structure that the surfactant will form in the vicinity of the DNA molecules.

The geometric forms that are available to a surfactant aggregate depend on the surfactant parameter,  $N_s$ . This can be described by  $v/la_0$ , where  $v$  and  $l$  stand for the volume and length

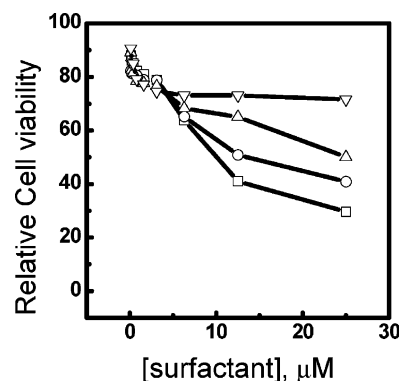


**Figure 7.** Effect of different surfactants on the viability of HeLa cells CTAB ( $\square$ ), S1 ( $\circ$ ), S2 ( $\triangle$ ), and S3 ( $\nabla$ ).

of the hydrocarbon chain, respectively, and  $a_0$  is the effective area per headgroup.<sup>55</sup> When  $N_s$  is close to unity the surfactants will usually form planar bilayers. Decreasing  $N_s$  will lead to the formation of surfactant aggregates with higher curvatures. In the surfactant systems considered in this work, when the substitution of the headgroup is performed,  $a_0$  can increase for two reasons: (i) simple geometry, since the methyl groups are being replaced for bulkier ones, and (ii) hydration, a more polar headgroup will be more hydrated and therefore have a larger effective size. It is, therefore, reasonable to expect an increase in the curvature of the surfactant aggregates. It should be noted that these arguments apply only for the case that the area is not mainly determined by electrostatic repulsions, like in the self-assembly of an ionic surfactant alone. On the other hand, the argument applies when the electrostatic interactions have been quenched like in the presence of high electrolyte concentrations or, as in our case, by an oppositely charged polelectrolyte.

The observation that surfactants with more hydrophilic headgroups compact DNA for the same concentrations as CTAB but expel ethidium bromide only at higher concentrations, and less efficiently, is understandable in terms of packing arguments. Whereas CTAB is known for forming rod-like micelles in the vicinity of DNA,<sup>56–58</sup> it is highly probable that by increasing the size of the headgroup the micelles formed in the DNA-surfactant complexes are smaller and more globular, which leads to a less efficient coverage, patch-like, of the DNA molecules, leaving parts of DNA open for ethidium bromide binding. Also the electrophoresis gel experiments give a good indication of a less efficient coverage of the DNA by the cationic surfactants with a larger number of hydroxyethyl groups. In case of S3, for example, although there is no migration of free DNA at ratios higher than 2.0, an intense fluorescence in the loading wells can still be observed at a 2.5 charge ratio.

However, our data does not provide a definite conclusion of which mode (weaker binding or less coverage) is the most correct for these systems. Structural studies, such as binary phase diagrams and aggregation number determinations, are currently being performed to unambiguously solve this problem.

**Cytotoxicity Studies.** We have performed cytotoxicity measurements to evaluate the cell viability in the presence of increasing concentrations of the four surfactants considered. As can be seen in Figure 7 the relative cell viability decreases with the increase in the concentration of surfactants. This is not surprising, what is interesting to note is that the cytotoxicity decreases substantially when increasing the number of the hydroxyl substitutions on the surfactant headgroup. With the addition of  $25 \mu\text{M}$  of CTAB for example, the relative cell viability decreases to 30%; however, the S3 surfactant shows a

much slower decay, reaching a plateau for around 70% of relative cell viability.

This can be promising for gene delivery applications. It has recently been shown that the precompaction of DNA with amino acid-based cationic surfactants increases the transfection efficiency of commercially available liposome formulations.<sup>59</sup> The fact that the most hydrophilic surfactants used in this study present little cytotoxicity make them candidates as potential precompaction agents. It is believed that transfection is limited by complex dissociation in the cytoplasm, or at least, by the accessibility of DNA. For example, lipoplexes (DNA–liposome complexes) made from liposomes with too high charge density present a lower transfection efficiency even though the complexes are successfully incorporated in the cells and escape from the endosomal membranes.<sup>45</sup> The S3 surfactant, for example, could be potentially used as a precompactant agent in the lipoplex preparation for gene delivery. Low concentrations are required for compacting DNA, and it is not substantially toxic to cells; also, it would presumably allow accessibility to the DNA from the cell machinery, once released from the liposomal complex.

## Conclusion

Here we describe a biophysical study of the interaction between DNA and surfactant molecules with varied architecture. The architecture was altered by substituting the methyl group of the CTAB headgroup sequentially with hydroxyethyl groups. It was shown that the formation of DNA–surfactant complexes is not dependent on the architecture of the surfactant headgroup. However, the accessibility to DNA by ethidium bromide is preserved to a certain extent, for the more hydrophilic surfactants. This can be due to a weakening of the interaction or to the structures that the surfactants form in the vicinity of the DNA; surfactants with more hydroxyethyl groups have a larger headgroup and can form smaller micellar aggregates with higher curvatures that lead to a less efficient coverage of the surface of DNA. However, our data does not give enough evidence for one or the other hypothesis.

The fact that these surfactants present a lower cytotoxicity makes them promising precompactant agents of DNA for gene delivery applications.

**Acknowledgment.** A.D.G. acknowledges the CSIR, Government of India, for Research Fellowships. Financial support from the Department of Science and Technology, Government of India, New Delhi to S.M. and P.K.D. is also gratefully acknowledged. R.S.D., M.G.M., and B.L. acknowledge Fundação para a Ciência e Tecnologia (FCT), Portugal (Projects POCTI/QUI/45344/2002 and POCI/QUI/58689/2004 and Grant SFRH/BPD/24203/2005). Authors acknowledge Swedish International Development Cooperation Agency (SIDA) for financial support.

## References and Notes

- Gershon, H.; Ghirlando, R.; Guttman, S. B.; Minsky, A. *Biochemistry* **1993**, *32*, 7143–7151.
- Melnikov, S. M.; Sergeev, V. G.; Yoshikawa, K. *J. Am. Chem. Soc.* **1995**, *117*, 2401–2408.
- Felgner, P. L.; Gadek, T. R.; Hom, M.; Roman, R.; Chan, H. W.; Wenz, M.; Northrop, J. P.; Ringold, G. M.; Danielsen, M. *Proc. Natl. Acad. Sci. U.S.A.* **1987**, *84*, 7413–7417.
- Xu, Y. H.; Szoka, F. C. *Biochemistry* **1996**, *35*, 5616–5623.
- McLoughlin, D. M.; O'Brien, J.; McManus, J. J.; Gorelov, A. V.; Dawson, K. A. *Bioseparation* **2000**, *9*, 307–313.
- Reimer, D. L.; Zhang, Y. P.; Kong, S.; Wheeler, J. J.; Graham, R. W.; Bally, M. B. *Biochemistry* **1995**, *34*, 12877–12883.

- Wong, F. M. P.; Reimer, D. L.; Bally, M. B. *Biochemistry* **1996**, *35*, 5756–5763.
- Ganguli, M.; Jayachandran, K. N.; Maiti, S. *J. Am. Chem. Soc.* **2004**, *126*, 26–27.
- Farhood, H.; Serbina, N.; Huang, L. *Biomembranes* **1995**, *1235*, 289–295.
- Zhu, N.; Liggitt, D.; Liu, Y.; Debs, R. *Science* **1993**, *261*, 209–211.
- Gao, X.; Huang, L. *Biochemistry* **1996**, *35*, 1027–1036.
- Bell, P. C.; Bergsma, M.; Dolbnya, I. P.; Bras, W.; Stuart, M. C. A.; Rowan, A. E.; Feiters, M. C.; Engberts, J. *J. Am. Chem. Soc.* **2003**, *125*, 1551–1558.
- VanDerWoude, I.; Wagenaar, A.; Meekel, A. A. P.; TerBeest, M. B. A.; Ruiters, M. H. J.; Engberts, J.; Hoekstra, D. *Proc. Natl. Acad. Sci. U.S.A.* **1997**, *94*, 1160–1165.
- Lander, R. J.; Winters, M. A.; Meacle, F. J.; Buckland, B. C.; Lee, A. L. *Biotechnol. Bioeng.* **2002**, *79*, 776–784.
- Macfarlane, D. E.; Dahle, C. E. *Nature* **1993**, *362*, 186–188.
- Macfarlane, D. E.; Dahle, C. E. *J. Clin. Lab. Anal.* **1997**, *11*, 132–139.
- Hamel, A. L.; Wasylyshen, M. D.; Nayar, G. P. S. *J. Clin. Microbiol.* **1995**, *33*, 287–291.
- Rosa, M.; Dias, R.; Miguel, M. D.; Lindman, B. *Biomacromolecules* **2005**, *6*, 2164–2171.
- Dias, R. S.; Innerlohinger, J.; Glatter, O.; Miguel, M. G.; Lindman, B. *J. Phys. Chem. B* **2005**, *109*, 10458–10463.
- Dias, R.; Mel'nikov, S.; Lindman, B.; Miguel, M. G. *Langmuir* **2000**, *16*, 9577–9583.
- Dias, R. S.; Lindman, B.; Miguel, M. G. *J. Phys. Chem. B* **2002**, *106*, 12608–12612.
- Cardenas, M.; Dreiss, C. A.; Nylander, T.; Chan, C. P.; Cosgrove, T.; Lindman, B. *Langmuir* **2005**, *21*, 3578–3583.
- Barreleiro, P. C. A.; Lindman, B. *J. Phys. Chem. B* **2003**, *107*, 6208–6213.
- Zhu, D. M.; Evans, R. K. *Langmuir* **2006**, *22*, 3735–3743.
- Ewert, K. K.; Evans, H. M.; Zidovska, A.; Bouxsein, N. F.; Ahmad, A.; Safinya, C. R. *J. Am. Chem. Soc.* **2006**, *128*, 3998–4006.
- Marchetti, S.; Onori, G.; Cametti, C. *J. Phys. Chem. B* **2005**, *109*, 3676–3680.
- Zhou, S. Q.; Liang, D. H.; Burger, C.; Yeh, F. J.; Chu, B. *Biomacromolecules* **2004**, *5*, 1256–1261.
- Spink, C. H.; Chaires, J. B. *J. Am. Chem. Soc.* **1997**, *119*, 10920–10928.
- Nisha, C. K.; Manorama, S. V.; Ganguli, M.; Maiti, S.; Kizhakke-dathu, J. N. *Langmuir* **2004**, *20*, 2386–2396.
- Matsuzawa, Y.; Kanbe, T.; Yoshikawa, K. *Langmuir* **2004**, *20*, 6439–6442.
- Fischer, D.; von Harpe, A.; Kunath, K.; Petersen, H.; Li, Y. X.; Kissel, T. *Bioconjugate Chem.* **2002**, *13*, 1124–1133.
- Wolfert, M. A.; Dash, P. R.; Nazarova, O.; Oupicky, D.; Seymour, L. W.; Smart, S.; Strohal, J.; Ulbrich, K. *Bioconjugate Chem.* **1999**, *10*, 993–1004.
- Wink, T.; de Beer, J.; Hennink, W. E.; Bult, A.; van Bennekom, W. P. *Anal. Chem.* **1999**, *71*, 801–805.
- Bronich, T.; Kabanov, A. V.; Marky, L. A. *J. Phys. Chem. B* **2001**, *105*, 6042–6050.
- Cui, L.; Miao, J. J.; Zhu, L. *Macromolecules* **2006**, *39*, 2536–2545.
- Caracciolo, G.; Pozzi, D.; Amenitsch, H.; Caminiti, R. *Langmuir* **2005**, *21*, 11582–11587.
- Osfouri, S.; Stano, P.; Luisi, P. L. *J. Phys. Chem. B* **2005**, *109*, 19929–19935.
- Hayakawa, K.; Santerre, J. P.; Kwak, J. C. T. *Biophys. Chem.* **1983**, *17*, 175–181.
- Izumrudov, V. A.; Zhiryakova, M. V.; Goulko, A. A. *Langmuir* **2002**, *18*, 10348–10356.
- Lima, M. C. P.; Neves, S.; Filipe, A.; Düzgünes, N.; Simões, S. *Curr. Med. Chem.* **2003**, *10*, 1221–1231.
- Niculescu-Duvaz, D.; Heyes, J.; Springer, C. *J. Curr. Med. Chem.* **2003**, *10*, 1233–1261.
- Zhang, S. B.; Xu, Y. M.; Wang, B.; Qiao, W. H.; Liu, D. L.; Li, Z. S. *J. Controlled Release* **2004**, *100*, 165–180.
- Moghimi, S. M. *Biomaterials* **2006**, *27*, 136–144.
- Ahmad, A.; Evans, H. M.; Ewert, K.; George, C. X.; Samuel, C. E.; Safinya, C. R. *J. Gene Med.* **2005**, *7*, 739–748.
- Lin, A. J.; Slack, N. L.; Ahmad, A.; George, C. X.; Samuel, C. E.; Safinya, C. R. *Biophys. J.* **2003**, *84*, 3307–3316.
- Bradley, A. J.; Devine, D. V.; Ansell, S. M.; Janzen, J.; Brooks, D. E. *Arch. Biochem. Biophys.* **1998**, *357*, 185–194.
- Woodle, M. C. *Adv. Drug Delivery Rev.* **1995**, *16*, 249–265.
- Sambrook, J.; Fritsch, E. F.; Maniatis, T. *Molecular Cloning: a laboratory manual*; Cold Spring Harbor Laboratory Press: New York, 1989.

- (49) Das, D.; Das, P. K. *Langmuir* **2003**, *19*, 9114–9119.
- (50) Holmberg, K.; Jönsson, B.; Kronberg, B.; Lindman, B. *Surfactants and Polymers in Aqueous Solution*, 2nd. ed.; John Wiley & Sons, Ltd.: New York, 2003.
- (51) Shinoda, K.; Nakagawa, T.; Tamamushi, B.-I.; Isemura, T. *Colloidal Surfactants, Some Physicochemical Properties*; Academic Press: London, 1963.
- (52) Kondo, Y.; Yokochi, E.; Mizumura, S.; Yoshino, N. *J. Fluorine Chem.* **1998**, *91*, 147–151.
- (53) Olins, D. E.; Olins, A. L.; Vonhippe, Ph. *J. Mol. Biol.* **1967**, *24*, 157–176.
- (54) Inoue, S.; Ando, T. *Biochemistry* **1970**, *9*, 388–394.
- (55) Evans, D. F.; Wennerström, H. *The Colloidal Domain. Where physics, chemistry and biology, and technology meet*, 2nd ed.; Wiley-VCH: New York, 1999.
- (56) Ghirlando, R.; Wachtel, E. J.; Arad, T.; Minsky, A. *Biochemistry* **1992**, *31*, 7110–7119.
- (57) Dias, R. S.; Lindman, B.; Miguel, M. G. *Prog. Colloid Polym. Sci.* **2001**, *118*, 163–167.
- (58) Leal, C.; Wadsö, L.; Olofsson, G.; Miguel, M.; Wennerström, H. *J. Phys. Chem. B* **2004**, *108*, 3044–3050.
- (59) Rosa, M.; Pereira, N. P.; Simões, S.; Lima, M. C. P.; Lindman, B.; Miguel, M. submitted.